RM No. L9B25b

NACA

RESEARCH MEMORANDUM

CONTINUATION OF WING FLUTTER INVESTIGATION IN THE TRANSONIC RANGE AND PRESENTATION OF A LIMITED SUMMARY OF FLUTTER DATA

By

William T. Lauten, Jr., and J. G. Barmby

Langley Aeronautical Laboratory
Langley Air Force Base, Va.

NATIONAL ADVISORY COMMITTEE FOR AERONAUTICS

WASHINGTON
April 21, 1949
Declassified December 14, 1953

NATIONAL ADVISORY COMMITTEE FOR AERONAUTICS

RESEARCH MEMORANDUM

CONTINUATION OF WING FLUTTER INVESTIGATION IN THE TRANSONIC RANGE AND PRESENTATION OF A LIMITED SUMMARY OF FLUTTER DATA

By William T. Lauten, Jr., and J. G. Barmby

SUMMARY

As a continuation of the program for flutter investigation in the transonic speed range two more freely falling bodies have been dropped and the results are reported herein. The two wings attached to the FB-5, which were designed to investigate the low supersonic region, remained intact up to $M = 0.86$ at which time the telemeter system became inoperative. One of the two wings attached to the FB-6 fluttered at a Mach number of 1.17 in a first-bending torsion mode. A comparison of the experimental flutter speed with the subsonic flutter theory for two-dimensional, incompressible flow shows the theory to be conservative and a comparison with linearized, two-dimensional supersonic flutter theory shows that it is also conservative.

Opportunity is also taken in this paper to present a limited summary of subsonic and supersonic data which indicates that, for an airplane traveling in a medium of essentially constant temperature and density, the region around $M = 0.9$ is the critical flutter region.

INTRODUCTION

Freely falling bodies have proved to be a satisfactory means of obtaining transonic flutter data. The method is reported in reference 1 and this paper is a continuation of the test program. Two more of these freely falling bodies, called flutter bombs, each carrying two unswept wings of semispan aspect ratio 3, were dropped from an altitude of approximately 35,000 feet. Employing a notation consistent with the earlier papers these two flutter bombs are designated here as the FB-5 and FB-6.

The two wings attached to the FB-5 were designed on the basis of previous experience to obtain flutter data at low supersonic speeds. Since in earlier drops the wing sections were of 9-percent thickness it was decided to make one wing, in this case wing 5001, a thin, 4-percent-thick section (NACA $65_{(09)}$A004) to note possible thickness effects. The other wing (5002, NACA 65A009) was designed with the center of gravity near the quarter-chord position in an attempt to avoid the coupled bending-torsion type of flutter and yield, if possible, a single degree of freedom or torsional flutter. Both wings had torsional stiffnesses comparable with the previous flutter-bomb wings.

The two identical FB-6 wings had NACA 65A009 sections. The wings were instrumented to indicate the flutter-mode shape. A high altitude for bomb release was chosen in an effort to get the wings through the high subsonic speed range at a low enough density to prevent flutter. The wings were of construction and properties similar to wing 2001 of reference 2 which was dropped from a lower altitude.

The primary purpose of this paper is to present the results obtained from the drop tests of these two flutter bombs. Opportunity is also taken to present a limited summary of subsonic and supersonic flutter data.

SYMBOLS

c wing chord, inches

l length of wing, inches

x_o distance of elastic axis behind leading edge, percent chord

x_1 distance of center of gravity behind leading edge, percent chord

M Mach number

M_{cr} theoretical Mach number at which sonic velocity is first attained over section of wing at zero lift

φ phase angle, wing torsional strain leading wing bending strain, degrees (reference 3)

A_g aspect ratio of one wing panel (l/c)

b semichord of test wing, feet

a nondimensional elastic-axis position, $\left(\frac{2x_o}{100} - 1\right)$

$a + x_\alpha$ nondimensional center-of-gravity position, $\left(\frac{2x_1}{100} - 1\right)$

ρ	air density, slugs per cubic foot
κ	ratio of mass of cylinder of testing medium of diameter equal to chord of wing to mass of wing, both taken for an equal length of span $\left(\frac{\pi\rho b^2}{m}\right)$
m	mass of wing per unit length
r_α	nondimensional radius of gyration about elastic axis $\left(\frac{I_\alpha}{mb^2}\right)$
I_α	polar moment of inertia about elastic axis (reference 3)
f_{h_1}	first bending natural frequency, cycles per second
f_{h_2}	second bending natural frequency, cycles per second
f_t	first torsion natural frequency, cycles per second
f_α	uncoupled first torsion frequency relative to elastic axis, cycles per second
g_h	structural damping coefficient in bending (reference 3)
g_α	structural damping coefficient in torsion (reference 3)
GJ	torsional rigidity, pound-inches^2
EI	bending rigidity, pound-inches^2
ω_α	torsional frequency, radians per second $\left(2\pi f_\alpha\right)$
t	time after release of missile from airplane, seconds
h	geometric altitude (distance above sea level), feet
p_s	static pressure, pounds per square foot
T	free-air temperature, $^{\circ}$F absolute
q	dynamic pressure, pounds per square foot
v	velocity, feet per second
V	velocity, miles per hour
V_e	experimental flutter velocity, miles per hour

V_R reference wing flutter velocity, based on theory of reference 3 for a two-dimensional unswept wing in an incompressible medium employing first bending frequency and uncoupled torsion frequency, miles per hour

V_D reference wing divergence speed, based on theory of reference 3 for a two-dimensional wing in an incompressible medium employing uncoupled torsion frequency, miles per hour

f_e experimental wing flutter frequency, cycles per second

f_R reference wing flutter frequency, cycles per second (analysis similar to that used in determining V_R)

APPARATUS AND METHODS

Models

Photographs and drawings of the complete FB-5 and FB-6 are shown in figures 1 and 2. The thin 5001 wing was made of solid dural with chordwise leading-edge and trailing-edge slits which were cut for the purpose of weakening the wing. These slits were covered with Scotch cellulose tape to preserve the airfoil shape. The other wings were of balsa with dural inserts. The wing parameters are listed in table I.

Instrumentation

Each of the four wings was equipped with strain gages and a break wire. The gages were mounted near the root to record both torsional and bending stresses on all wings except wing 6002, which was equipped with torsion gages only. Wing 6001 had, in addition to the root gages, a second set of bending gages mounted near the position of the second-bending node. A longitudinal and a vertical accelerometer were mounted at approximately the center-of-gravity position of the bomb. Signals from the strain gages, accelerometers, and break wires were transmitted over six telemeter channels simultaneously to two receiving stations. Telemeter data, time of release, and altitude and speed of the airplane were recorded or determined as reported in reference 2.

Measurements

In addition to telemeter data, measurements similar to those reported in reference 1 were taken of ground parameters and of atmospheric and flight conditions.

Reduction of Data

The reduction of principal data is similar to that reported in reference 1. Flutter was indicated when the signal from the strain gages increased rapidly in amplitude and also by the fact that, on those records which had signals from both bending and torsion gages, the oscillations were of the same frequency. Associated conditions were determined from the time-history curves. The phase angles between the bending and twisting of the wings were determined from the telemetered strain records in accordance with the sign convention for bending and twisting of reference 3. For definiteness, these angles are recorded in this paper as torsion strain leading bending strain.

RESULTS AND DISCUSSION

The time histories of the falls of the two flutter bombs are shown in figures 3 and 4. In these figures the variation of the bomb altitude, velocity, and Mach number with time are plotted together with the free-air static pressure and temperature corresponding to the geometric altitude of the bomb.

The signals transmitted from the FB-5 were extremely erratic; however, it appears that both wings remained on the bomb without flutter up to a Mach number of 0.86, at which time the telemeter ceased to function completely and no further information was obtained. The conditions at time of telemeter failure are listed in table II.

In the test of the FB-6 flutter was obtained on one wing. The other wing remained on the bomb for the duration of the fall. The data at flutter and at impact are listed in detail in table II. Flutter started at $M = 1.17$ and the telemeter record indicated that it was a bending-torsion type.

It is noted that wings 6001 and 6002 were designed with parameters similar to those of wing 2001 (reference 2) as evidenced by the fact that the reference flutter speed of wing 6001 was 485 miles per hour and that of wing 2001 was 474 miles per hour, both based on standard air density. As given in reference 2 wing 2001 (flutter bomb FB-2), which was dropped from 20,000 feet, fluttered at a Mach number of 0.84; whereas, in the present case, the FB-6 was dropped from 35,000 feet and wing 6001 fluttered at Mach number of 1.17. Clearly, because of the difference in the initial conditions, wing 6001 passed through the $M = 0.84$ range at such a low density that the dynamic pressure was not sufficient to produce flutter.

A comparison of the experimental flutter speed V_e and the reference flutter speed V_R based on the incompressible theory of reference 3 shows that the ratio $\frac{V_e}{V_R} = 1.86$. This result is in accord with similar results obtained from flutter tests at well-developed supersonic speeds ($M = 1.3$) reported in reference 4. In the experiments of this reference, the values of the ratio V_e/V_R were between 1.5 and 2.1, with one point at 2.58. It should be clearly understood that the two-dimensional incompressible theory of reference 3 is not expected to agree with three-dimensional compressible experiments. It is used as a convenient standard by which wings of different parameters may be compared and is especially valuable for this purpose in the mixed-flow region where none of the existing theories hold. It is also valuable to designers of transonic wings in that it gives them an easily calculated value which they may use as a criterion on which to base designs.

Figure 5 shows the experimental flutter point superposed on a plot of numerical values, based on parameters of wing 6001 at time of flutter, obtained from the two-dimensional subsonic theory of references 3 and 5 and the linearized, two-dimensional supersonic theory of reference 6. The theoretical curves are calculated employing first bending, first torsion, and zero damping. It may be seen that the supersonic theory gives only a slightly higher value for the flutter-speed coefficient than the subsonic theory at the lower supersonic Mach numbers ($M < 1.25$), but for higher Mach numbers the theoretical flutter-speed coefficient increases rapidly and for wing 6001 approaches infinity at $M = 1.43$. As pointed out in reference 4, the preliminary tests in more well-developed supersonic flow at $M = 1.3$ compare satisfactorily with the supersonic theory. However, at low supersonic speeds with round-nose airfoils, similar to those on the FB-6, the flow is probably mixed subsonic and supersonic so that the two-dimensional supersonic theory cannot be expected to apply. In addition, aspect-ratio effects may account for some of the discrepancy between experiment and theory. The single test point at

at $M = 1.17$ yields a value of $\frac{V_e}{V_{theory}} = 1.67$.

It is thought to be appropriate to include in this paper a limited amount of flutter data obtained over a range of Mach numbers on wings similar to wing 6001. These include some unpublished results from the Langley flutter tunnel, previous bomb drops (reference 2), the Langley supersonic flutter apparatus (reference 4), and rocket flights (reference 7). Some of these data are shown in figure 6. The test points presented are flutter points from wings which had approximately the same major parameters. All wings were unswept, had semispan aspect ratios ranging from 2 to 3.5, center-of-gravity locations between 43.7 and 49.6 percent chord, elastic axes between 30 and 50 percent chord and wing-density parameters $1/\kappa$ of 30 to 60. The data therefore represent a composite picture of a variety of airfoils tested under conditions which differ widely. The two-dimensional, incompressible theory of reference 3 is used for convenience as a basis of the comparison, particularly since there is no basic theory for predicting flutter speed in the mixed-flow or transonic speed range. The reference flutter velocity V_R was determined for each wing and the ratio V_e/V_R is plotted against Mach number in figure 6. The plot shows that in the subsonic range there is only a small difference between the experimental and theoretical values. This difference is of the order expected because of aspect-ratio and compressibility effects. Above $M = 0.9$ and on up to the limit of the experiments, the incompressible reference velocity is conservative by increasingly larger amounts.

The flutter behavior in the region of Mach numbers around unity is determined by the flight history of the vehicle. This may be explained as follows: If a wing is subjected to an increase in velocity in a medium of essentially constant temperature and density, such as that encountered by a low-altitude rocket, the plot of V/V_R against Mach number is essentially a straight line which passes through the origin. Now let it be assumed that a wing attached to a rocket vehicle has such characteristics that the aforementioned line representing its flight path is tangent to the experimental flutter curve as shown in figure 6. It may be seen that the point of tangency of this line with the experimental flutter curve is approximately $M = 0.9$ and thus the critical flutter region may be defined as the region around $M = 0.9$. Similar considerations are made in connection with figure 17 of reference 6. If the vertical distance between the line representing the flight path and the experimental flutter curve is considered to correspond to a margin of safety, it may be seen that, with reference to the point of tangency, the margin of safety increases as the Mach number increases or decreases. If the reference flutter velocity is increased by making the wing slightly stiffer in torsion the slope of the line representing the flight path is decreased, the line is no longer tangent to the flutter curve, and flutter will be prevented. For this particular type of flutter curve the approximate-straight-line path of the rocket implies that the flutter condition would be first reached at Mach numbers lower than those of the critical flutter region.

On the other hand, as shown in figure 6, the corresponding flight history of the bomb drop is a curved line. For this type of curve there exists the possibility of obtaining flutter above the critical region. In the case of the FB-6, it may be seen that the critical region for the rockets is avoided because the flight history of the bomb is changed by the fact that it commences its flight in a medium of low density and the reference flutter velocity is constantly decreasing as the bomb nears the ground. The flutter region for the bomb may also be moved to a higher Mach number range by making the wing stiffer, as in the case of the rocket.

It should be emphasized that the experimental flutter curve in figure 6 is taken from a series of wings whose center-of-gravity positions are approximately 45 percent chord and whose semispan aspect ratios are approximately 3. This experimental flutter curve therefore is a particular curve and is not applicable to wings in general, particularly in the supersonic range where a small change in the center-of-gravity position has a large effect on the flutter speed (reference 4). It should be further pointed out, as indicated in some unpublished work in the Langley flutter tunnel, that as the aspect ratio is increased the margin of safety in the subsonic region may decrease and for high aspect ratios the ratio V_e/V_R may be slightly less than unity at higher subsonic Mach numbers. However, for the purpose of making preliminary estimates of a wing flutter speed in the transonic speed range a curve similar to figure 6, used in conjunction with the two-dimensional subsonic theory of reference 3, is of practical value.

CONCLUDING REMARKS

The two wings attached to the FB-5, which were designed to investigate the low supersonic region, remained intact on the bomb up to a Mach number of 0.86, at which point the telemeter system became inoperative. One of the two wings attached to the FB-6 fluttered at a Mach number of 1.17 in a low-bending torsion mode. The experimental flutter speed exceeds the incompressible-flow reference flutter speed of NACA Rep. No. 685 by 87 percent, which is in accord with the tests in the supersonic flutter apparatus at $M = 1.3$ given in NACA RM No. L8J11. Although these tests in the well-developed supersonic flow at $M = 1.3$ compare favorably with the supersonic theory of NACA Rep. No. 846, the experimental flutter speed of this flutter-bomb test at a transonic Mach number of 1.17 exceeds the speed based on the linearized, two-dimensional theory by 67 percent.

Opportunity is taken herein to present a limited summary of subsonic and supersonic data on related wings which indicates that, for an airplane traveling in a medium of essentially constant temperature and density, the region around $M = 0.9$ is the critical flutter region.

Langley Aeronautical Laboratory
National Advisory Committee for Aeronautics
Langley Air Force Base, Va.

REFERENCES

1. Barmby, J. G., and Clevenson, S. A.: Initial Test in the Transonic Range of Four Flutter Airfoils Attached to a Freely Falling Body. NACA RM No. L7B27, 1947.

2. Clevenson, S. A., and Lauten, William T., Jr.: Flutter Investigation in the Transonic Range of Six Airfoils Attached to Three Freely Falling Bodies. NACA RM No. L7K17, 1948.

3. Theodorsen, Theodore, and Garrick, I. E.: Mechanism of Flutter - A Theoretical and Experimental Investigation of the Flutter Problem. NACA Rep. No. 685, 1940.

4. Tuovila, W. J., Baker, John E., and Regier, Arthur A.: Initial Experiments on Flutter of Unswept Cantilever Wings at Mach Number 1.3. NACA RM No. L8J11, 1948.

5. Garrick, I. E.: Bending-Torsion Flutter Calculations Modified by Subsonic Compressibility Corrections. NACA Rep. No. 836, 1946.

6. Garrick, I. E., and Rubinow, S. I.: Flutter and Oscillating Air-Force Calculations for an Airfoil in a Two-Dimensional Supersonic Flow. NACA Rep. No. 846, 1946.

7. Barmby, J. G., and Teitelbaum, J. M.: Initial Flight Tests of the NACA FR-2, a High-Velocity Rocket-Propelled Vehicle for Transonic Flutter Research. NACA RM No. L7J20, 1948.

TABLE I

WING PARAMETERS

Parameter	Wing			
	5001	5002	6001	6002
Airfoil Section	NACA $65_{(09)}$A004	NACA 65A009	NACA 65A009	NACA 65A009
M_{cr}	0.88	0.8	0.8	0.8
c	8	8	8	8
l	23.75	24	23.5	23.5
A_g	2.97	3	2.94	2.94
b	0.333	0.333	0.333	0.333
x_1	46.2	24.2	43.75	43.8
x_o	43.7	37.5	33.5	35.2
a	-0.126	-0.25	-0.33	-0.296
$a + x_\alpha$	-0.076	-0.516	-0.125	-0.124
$1/\kappa$ (stnd)	85.3	54	27.7	32.4
r_α^2	0.196	0.2139	0.345	0.2954
f_{h_1}	12	17	22.4	23
f_{h_2}	73	101	134	129.5
f_t	89.3	80	102	99.3
f_α	88.6	64.7	95.4	94
g_h	0.007	0.045	0.022	-------
g_α	0.035	0.067	0.015	0.016
GJ	95,800	28,000	63,500	75,500
EI	72,900	10,250	102,500	106,000

NACA

TABLE II

RESULTS OF DROPS

Parameter	Wing			
	5001 (a)	5002 (a)	6001 (b)	6002 (c)
M	0.86	0.86	1.17	1.168
V_e	-------	-------	880	-------
f_e	-------	-------	57.5	-------
V	609.5	609.5	880	901
ρ	0.00107	0.00107	0.00202	0.00233
q	427.5	427.5	782	945
1/κ	189.7	120.1	32.6	33.1
t	25.2	25.2	45.13	49.28
h	24,800	24,800	5300	0
T	450	450	509	534
p_s	825	825	1760	2125
φ	-------	-------	310	-------
V_R	796	∞	470	439
f_R	34.9	-------	58.8	55.5
V_D	891	662	783	660

[a]Condition at time of telemeter failure.

[b]Condition at time of flutter.

[c]Condition at time of impact with ground.

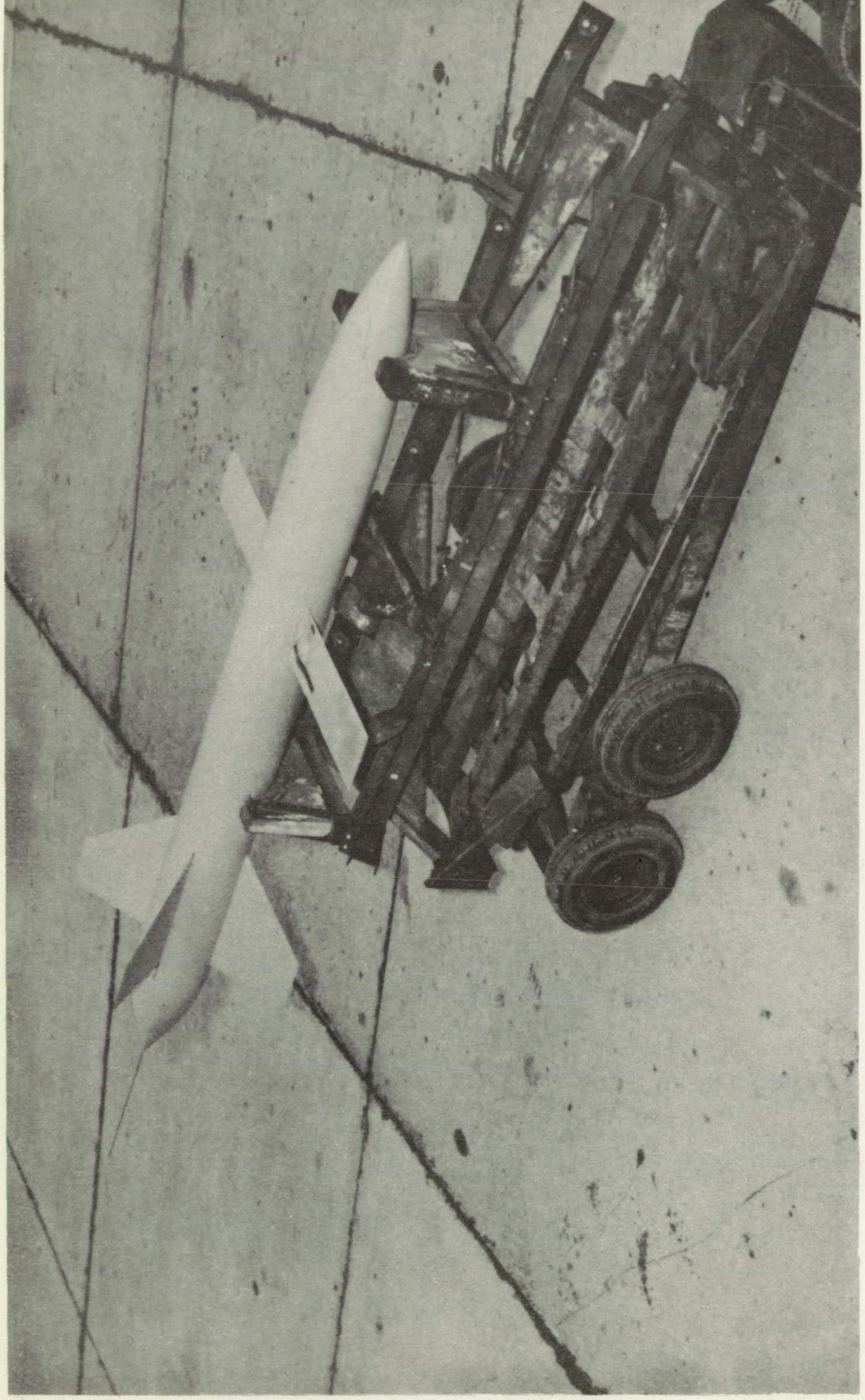

NACA L-57924

(a) Flutter bomb FB-5.

Figure 1.- Photographs of flutter bombs.

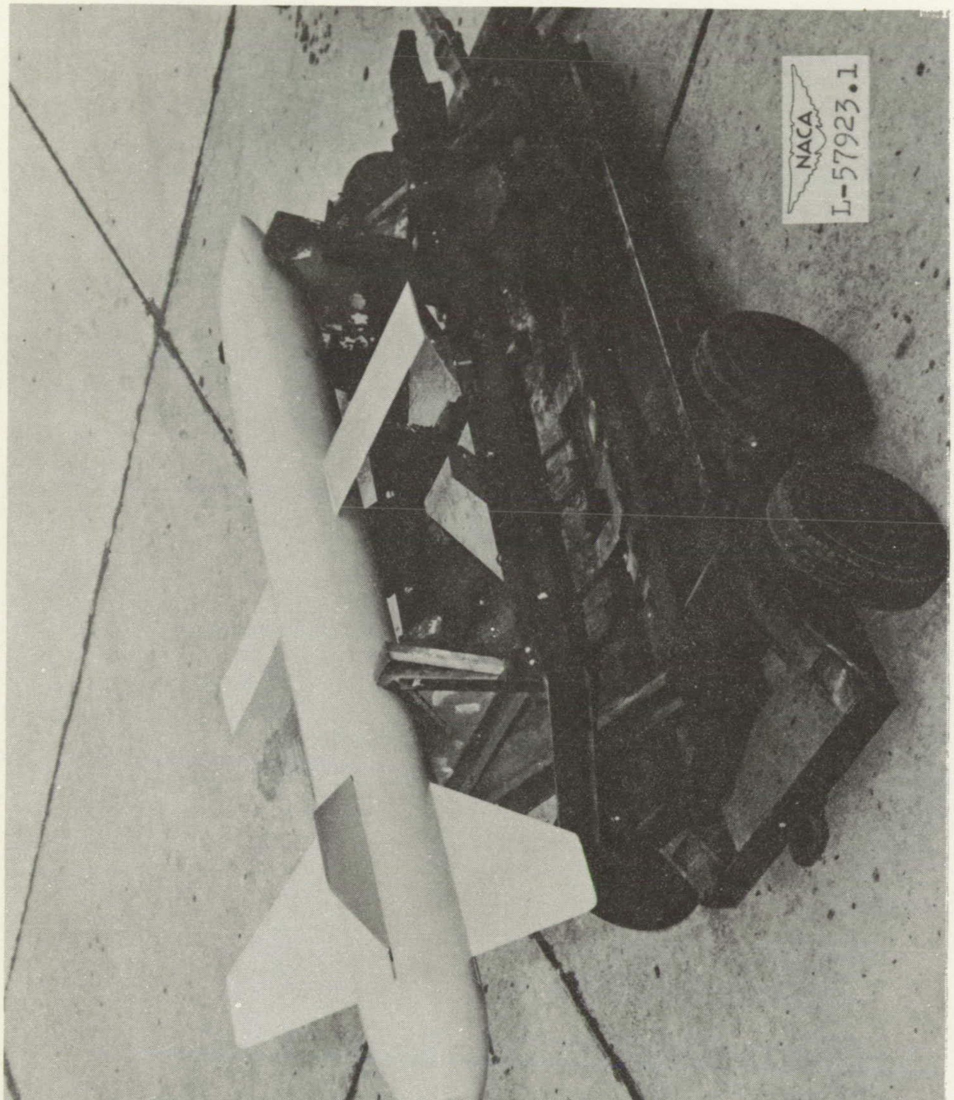

(b) Flutter bomb FB-6.

Figure 1.- Concluded.

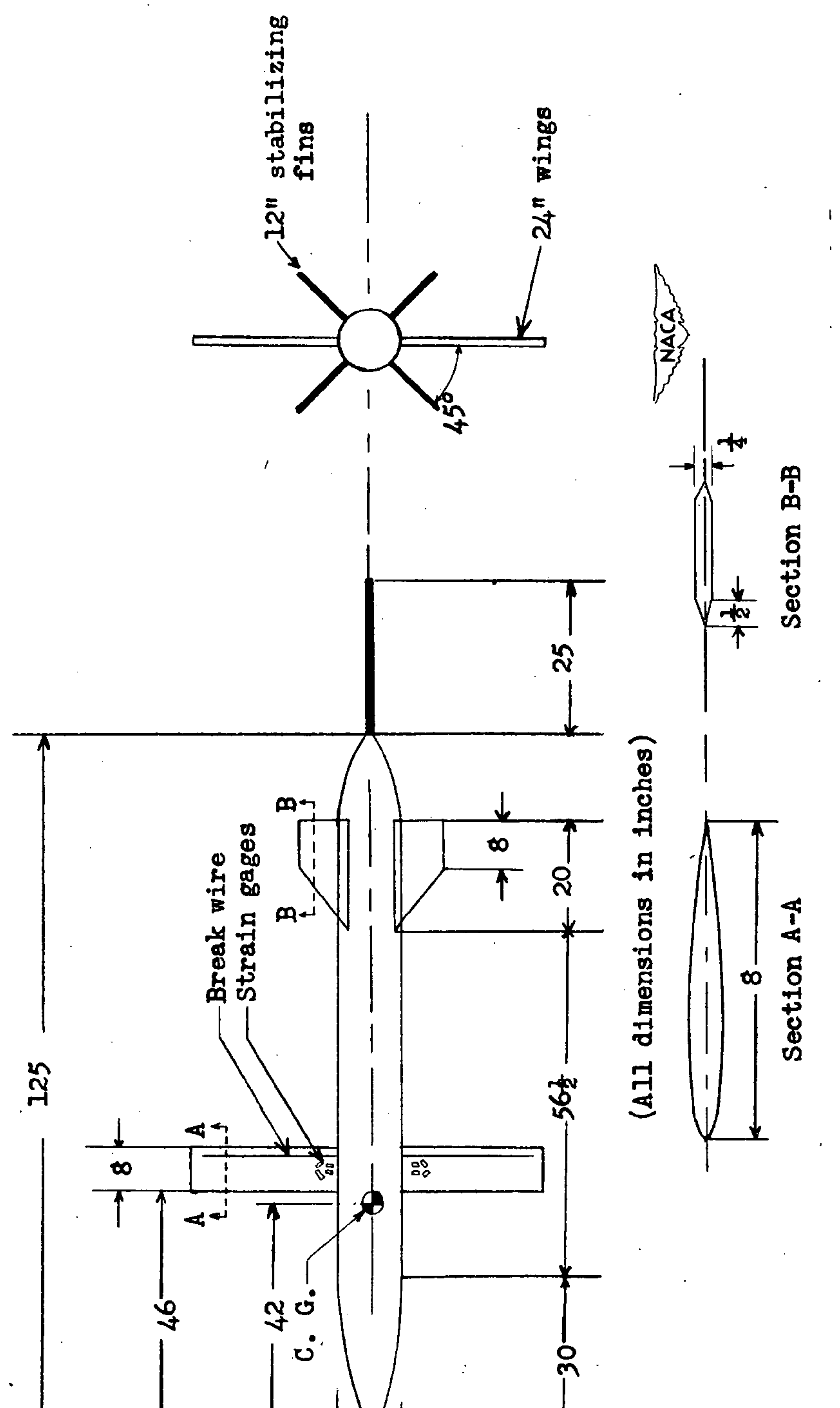

Figure 2.- Dimensional drawing of the FB-5 and FB-6.

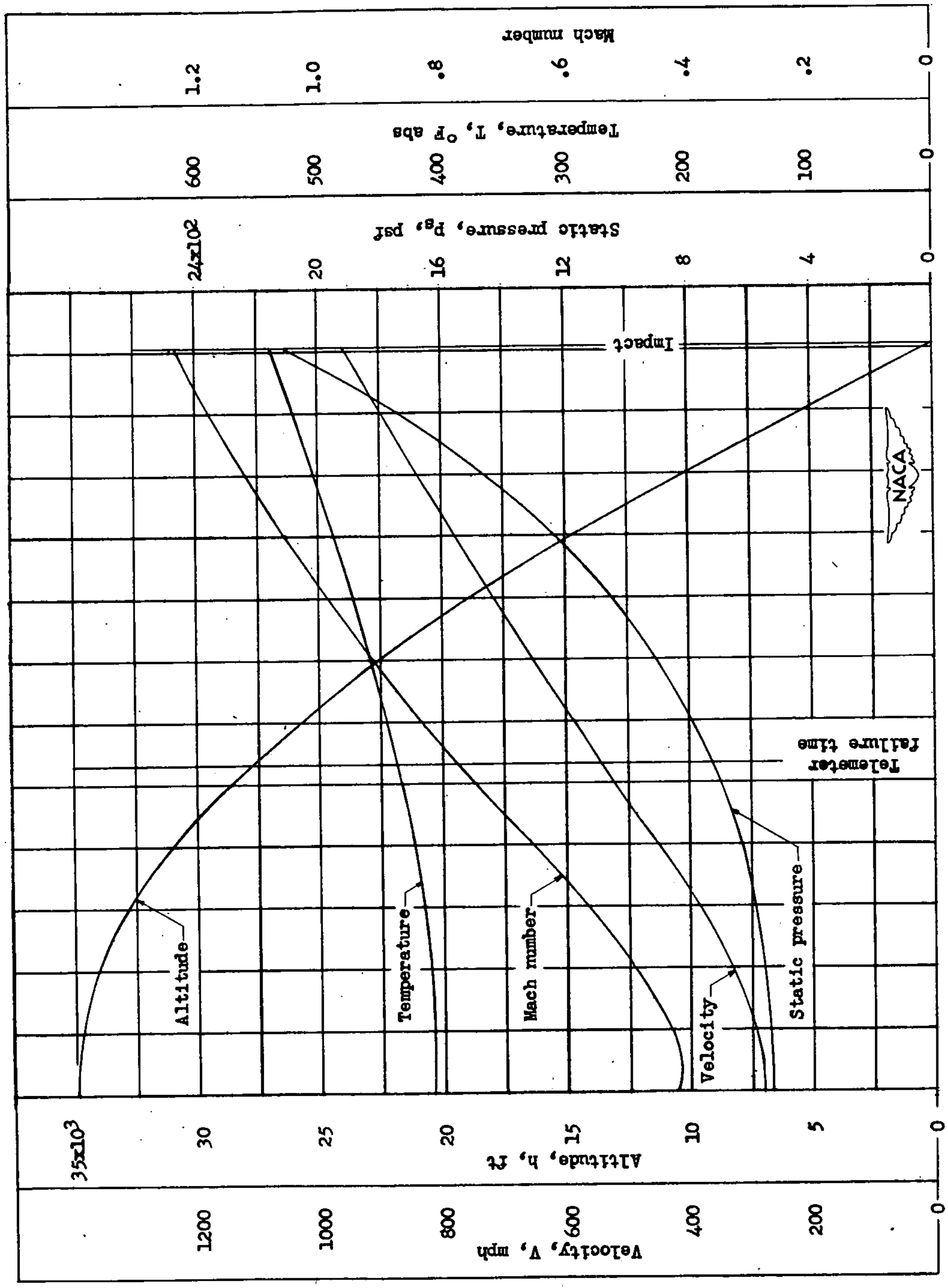

Figure 3.- Time history of fall of the FB-5.

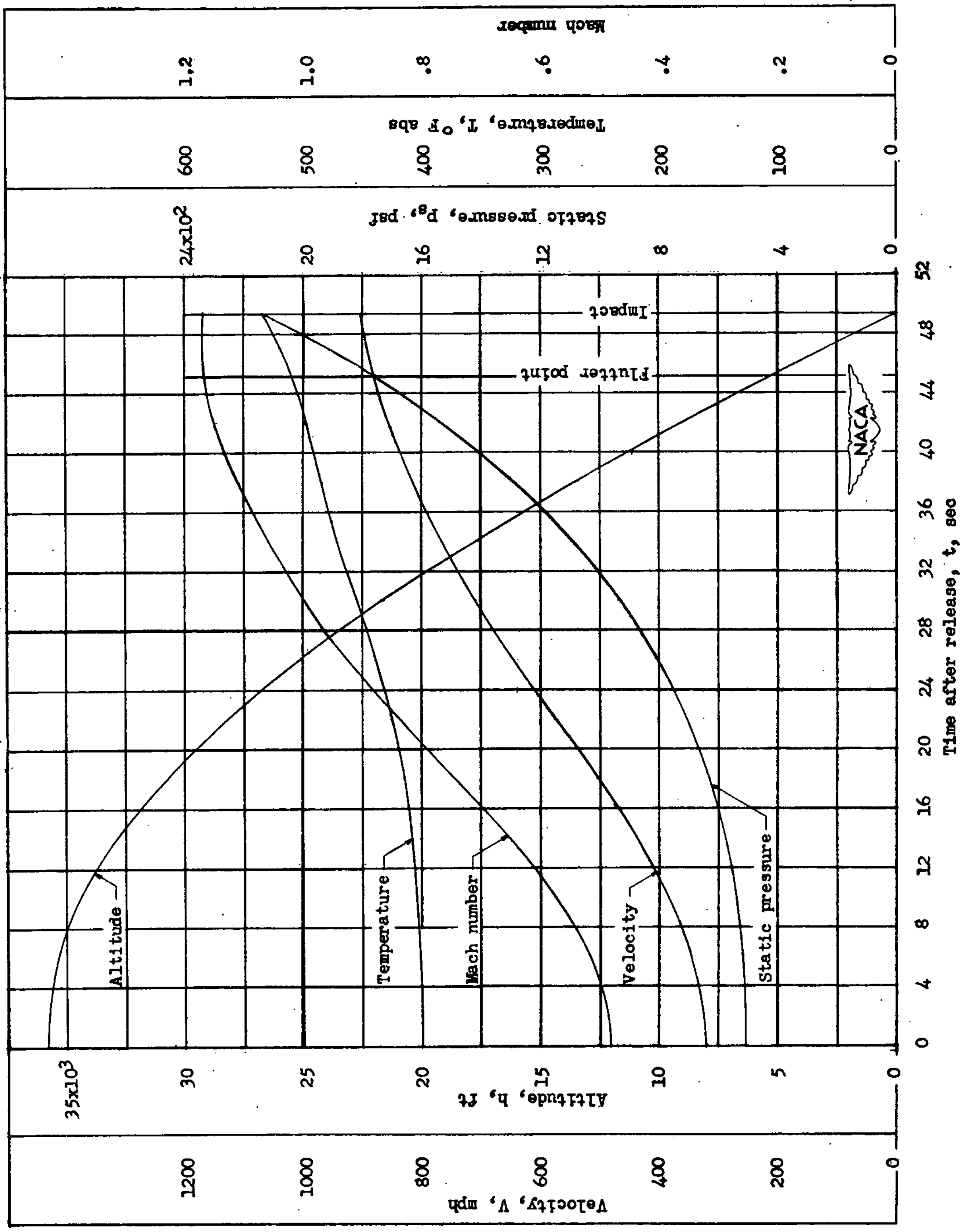

Figure 4.– Time history of fall of the FB-6.

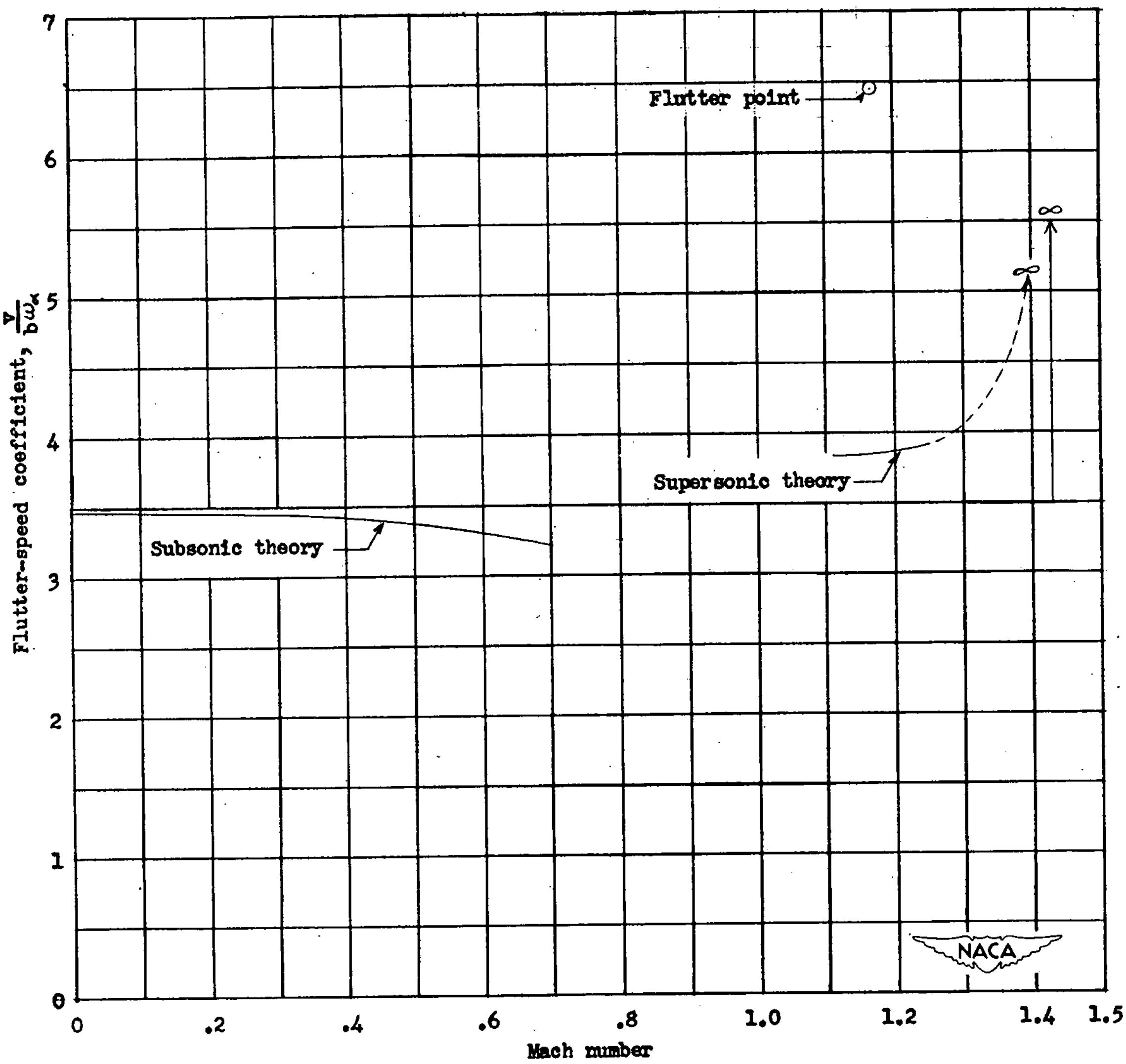

Figure 5.- Plot of flutter-speed coefficient against Mach number for wing 6001.

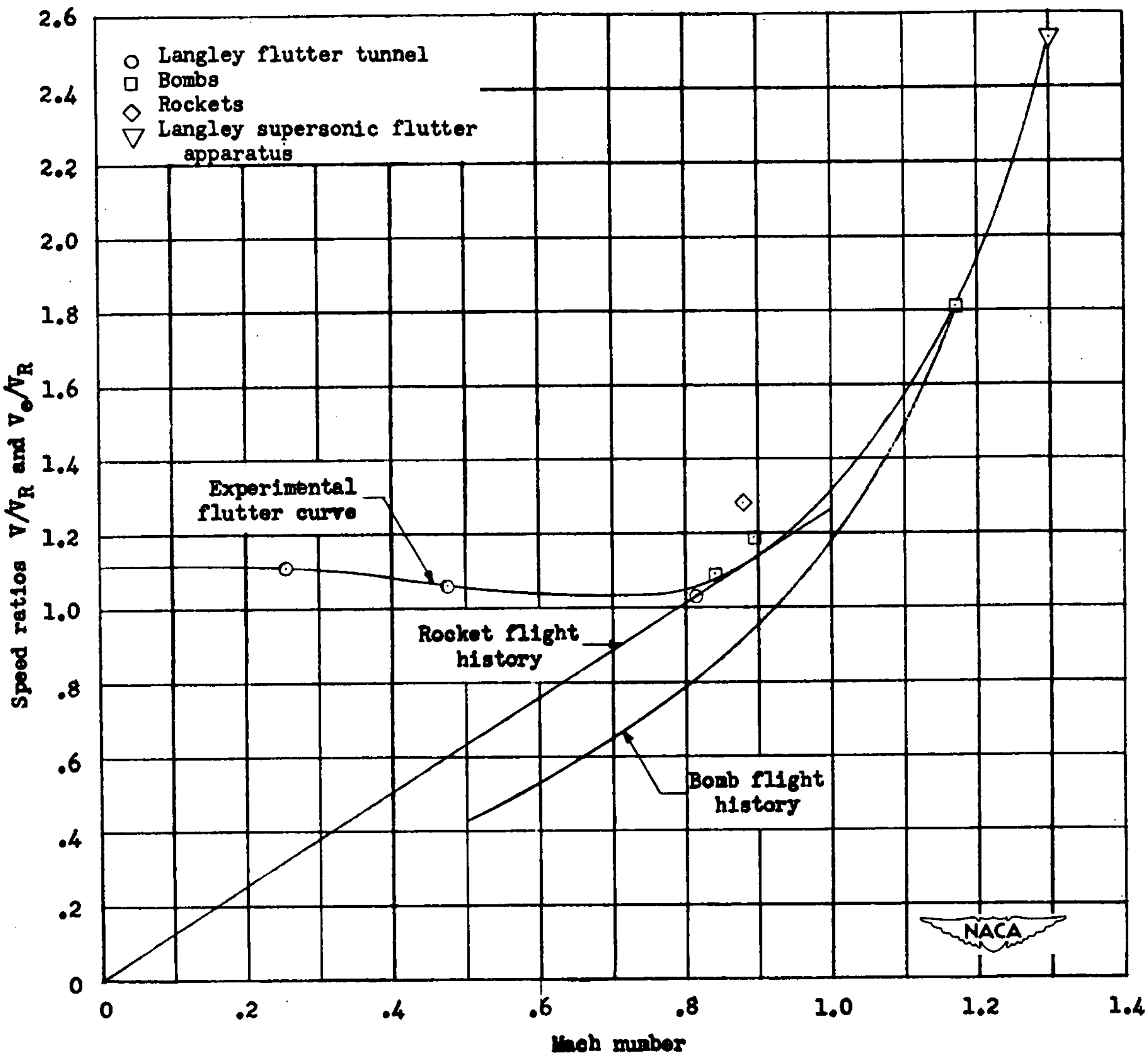

Figure 6.– Experimental flutter speed curve and a typical flight history of a rocket and a bomb.